Sensitivity of Tyrosyl Radical *g*-Values to Changes in Protein Structure: A High-Field EPR Study of Mutants of Ribonucleotide Reductase

Sun Un,*,† Catherine Gerez,‡ Eric Elleingand,‡ and Marc Fontecave‡

Contribution from the Département de Biologie Cellulaire et Moléculaire, Section de Bioénergétique, CNRS URA2096, CEA Saclay, F-91191 Gif-sur-Yvette, France, and Laboratoire de Chimie et Biochimie des Centres Redox Biochimiques, DBMS, CEA Grenoble, F-38054 Grenoble, France

Received October 11, 2000. Revised Manuscript Received December 22, 2000

Abstract: The local electrostatic environment plays a critical role in determining the physicochemical properties of reactive radicals in proteins. High-field electron paramagnetic resonance (HF-EPR) spectroscopy has been used to determine the sensitivity of the tyrosyl radical *g*-values to local electrostatic environment. Site-specific mutants of ribonucleotide reductase from *Escherichia coli* were used to study the effect of introducing a charge group on the HF-EPR spectrum of the stable tyrosyl (Y122) radical. The changes affected by the mutations were small, but measurable. Mutation of isoleucine-74 to an arginine (I74R) or lysine (I74K) induced disorder in the hyperfine interactions. Similar effects were observed for the mutation of valine-136 to an arginine (V136R) or asparagine (V136N). For five or six mutants studied, the g_x component of the **g**-tensor was distributed. For the isoleucine-74 to lysine (I74K) and leucine-77 to phenylalanine (L77F) mutants, a shift of 1×10^{-4} in g_x value was also detected. For the I74K mutant, it is shown that the shift is consistent with the introduction of a charged residue, but cannot be distinguished from changes in the electrostatic effect of the nearby diiron center. For the L77F mutant, the shift is induced by the diiron center. Using existing tyrosyl radical **g**-tensor measurements, we have developed a simple effective charge model that allows us to rationalize the effect of the local electrostatic environments in a number of proteins.

High magnetic-field electron paramagnetic resonance spectroscopy (HF-EPR) is becoming an increasingly important tool for studying organic radicals and in particular radicals in proteins. A diverse number of radicals, such as semiquinone,[1] carotenoid,[2] pheophytin,[1] chlorophyll,[3] nucleic acid,[4] and amino acid radicals,[5−8] have been investigated with this technique. There are essentially two driving forces behind this: resolution and accurate *g*-value measurements. In this paper, we focus on the latter. The *g*-values of radicals are in principle sensitive to the electronic structure of radicals. Hence, they provide a valuable probe for identifying radicals,[4] as well as studying radical−environment interactions.[5−7] By using HF-EPR, it is possible to measure *g*-values with unprecedented accuracy. A natural question that arises is how sensitive are the *g*-values of the organic radicals to the structure of the radical and its protein environment? In previous experimental studies, we have examined this question by comparing the HF-EPR spectra of tyrosyl radicals in several proteins. The *g*-values of tyrosyl radical were found sensitive to the local electrostatic environment. The *g*-anisotropies of tyrosyl radicals in plant photosystem II (PSII)[5] and bovine liver catalase (BLC)[6] are markedly different from each other and from that of ribonucleotide reductase (RNR)[7] from *Escherichia coli*. The *g*-values of the RNR tyrosyl radicals from different organisms show a large variation. Using computational approaches, we[5a] and others[9] have shown that these differences are correlated to variations in hydrogen bonding to the radicals. Several subsequent studies have used these results to rationalize *g*-values of tyrosyl radicals in other proteins.[5−7] The effect of hydrogen bonding is a special case of a more general electrostatic effect. For tyrosyl and semiquinone radicals, it can be shown that the g_x value can be

† CEA Saclay.

‡ CEA Grenoble.

(1) Dorlet, P.; Rutherford, A. W.; Un, S. *Biochemistry* **2000**, *39*, 7826−7834.

(2) Knonvalova, T. A.; Krystek, J.; Bratt, P. J.; van Tol, J.; Brunel, L.-C.; Kispert, L. D. *J. Phys. Chem. B* **1999**, *103*, 5782−5786. Lakshmi, K. V.; Reifler, M. J.; Brudvig, G. W.; Poluektov, O. G.; Wagner, A. M.; Thurnauer, M. C. *J. Chem. Phys. B* **2000**, *104*, 10445−10448. Faller, P.; Rutherford, W.; Un, S. *J. Chem. Phys. B* **2000**, *104*, 10960−10963.

(3) Bratt, P. J.; Poluekov, O. G.; Thurnauer, M. C.; Krzystek, J.; Brunel, L.-C.; Schrier, J.; Hsiao, Y.-W.; Zerner, M.; Angerhofer, A. *J. Chem. Phys. B* **2000**, *104*, 6973−6977.

(4) Lawrence, C. C.; Bennati, M.; Obias, H. V.; Bar, G.; Griffin, R. G.; Stubbe, J. *Proc. Natl. Acad. Sci. U.S.A.* **1999**, *96*, 8979−8984.

(5) (a) Un, S.; Atta M.; Fontecave, M.; Rutherford, A. W. *J. Am. Chem. Soc*. **1995**, *117*, 10713−10719. (b) Un, S.; Tang, X.-O.; Diner, B. A. *Biochemistry* **1996**, *35*, 679−684. (c) Farrar, C. T.; Gerfen, G. J.; Griffin, R. G.; Force, D. A.; Britt, R. D. *J. Phys. Chem. B* **1997**, *101*, 6634−6641.

(6) (a) Ivancich, A.; Mattioli, T. A.; Un, S. *J. Am. Chem. Soc.* **1999**, *121*, 5743−5753. (b) Ivancich, A.; Jouve, H. M.; Gaillard, J. *J. Am. Chem. Soc.* **1996**, *118*, 12852−12853.

(7) (a) Liu, A. M.; Barra, A.-L.; Rubin, H.; Lu, G. Z.; Gräslund, A. *J. Am. Chem. Soc.* **2000**, *122*, 1974−1978. (b) Liu, A.; Potsch, S.; Davydov, A.; Barra, A.-L.; Rubin, H.; Gräslund, A. *Biochemistry* **1998**, *37*, 16369−16377. (c) Elleingand, E.; Gerez, C.; Un, S.; Knupling, M.; Lu, G. Z.; Salem, J.; Rubin, H.; Sauge-Merle, S.; Laulhere, J. P.; Fontecave, M. *Eur. J. Biochem.* **1998**, *258*, 485−490. (d) van Dam, P. J.; Willems, J. P.; Schmidt, P. P.; Potsch, S.; Barra, A.-L.; Hagen, W. R.; Hoffman, B. M.; Andersson, K. K.; Gräslund, A. *J. Am. Chem. Soc.* **1998**, *120*, 5080−5085. (e) Allard, P.; Barra, AL; Andersson K. K.; Schmidt, P. P.; Atta, M.; Gräslund, A. *J. Am. Chem. Soc.* **1996**, *118*, 895−896.

(8) For other examples see: van der Donk, W. A.; Stubbe, *J. Chem. Rev.* **1998**, *98*, 705−762 and references therein. Kolberg, M.; Bleifuss, G.; Potsch, S.; Gräslund, A.; Lubitz, W.; Lassmann, G.; Lendzian, F. *J. Am.Chem. Soc.* **2000**, *122*, 9856−9857.

(9) Engström, M.; Himo, F.; Gräslund, A.; Minaev, B.; Vahtreas, O.; Agren, H. *J. Phys. Chem. A* **2000**, *104*, 5149−5153.

10.1021/ja003650b CCC: $20.00
Published on Web 03/07/2001

approximated by

$$\Delta g_x = g_x - g_e \approx \frac{2\zeta_O \rho_z \rho_y^*}{\Delta E_{n\pi^*}} \quad (1)$$

where ζ_O is the spin−orbital coupling constant of oxygen, ρ_z is the ground-state π spin density on the oxygen and ρ_y* is the oxygen p_y orbital contribution to the state corresponding to an excitation of an electron from the nonbonding molecular orbital centered on the oxygen to the singly occupied molecular orbital (SOMO), the excitation energy of which is $\Delta E_{n\pi^*}$.[10] The perturbative effect of the electrostatic environment can be included by adding a potential energy term, $\phi(r)$, in the denominator and a scaling factor, $k(r)$,[5a,11] in the numerator to account for modification in spin densities due to external charges. This leads to

$$\Delta g_x \approx \frac{2\zeta_O \rho_z \rho_y^* k(r)}{\Delta E_{n\pi^*} + \phi(r)} \approx \frac{2\zeta_O \rho_z \pi_y^* k(r)}{\Delta E_{n\pi^*}} \left(1 + \frac{C}{r^2} + \frac{D}{r^3} + \frac{E}{r^6}..\right) \quad (2)$$

For the case of modest to weak electrostatic interactions, the main effect on tyrosyl radicals is the change in energy of the nonbonding electrons and $k(r)$ is small. For a net electrically positive electrostatic effect, C and D are negative and E is negligible leading to smaller g_x values.[11,12]

One experimental approach to quantitatively assess the sensitivity of tyrosyl radical g-values is to use an in vitro model system that has a stable radical and an ionic group. Such an approach would entail synthesis and detailed structural characterization of the model system. An attractive alternative is to use site-specific mutants of the *E. coli* RNR. The structure of the wild-type protein is known.[13] Therefore, the protein provides a stable radical within a known structural framework. In a previous study, we used mutants of PSII to demonstrate the effect of hydrogen bonding on the g-values of the stable tyrosyl radical, Y_D.[5b] When the putative hydrogen-bond donor was changed to a non-hydrogen-bonding residue, the Y_D g-anisotropy increased to nearly that of the RNR. In this study, we have utilized mutants of RNR.

Ribonucleotide reductase is a complex enzyme essential to all living organisms. It catalyzes the reduction of ribonucleotides to deoxyribonucleotides which are required for DNA synthesis. The enzyme is a 1:1 complex of two homodimeric proteins, referred to commonly as R1 and R2. The R2 unit contains a dinuclear non-heme iron center and a stable tyrosyl radical (Y122) that is essential for enzymatic activity. The tyrosyl radical sits in a hydrophobic pocket. However, the phenoxyl oxygen of the radical is 5.34 Å away from the nearest iron atom of the binuclear metal center. This metal center along with its negatively charged ligands imposes a net electropositive environment on the tyrosyl radical.[5a]

A hydrophobic channel connects the radical to the protein surface. The channel consists of two layers of residues. The outer one is composed of valine-136 (V136), isoleucine-74 (I74), and valine-30 (V30) and the inner of valine-135 (V135), leucine-77 (L77), and isoleucine-126 (I126). The role of these residues in the transport of hydrophobic radical scavengers has been investigated. The L77 residue, which is within 5 Å of Y122, has been replaced by a larger phenylalanine to study steric effects. The crystallographic structure of this mutant has been determined.[14] The neutral V136 and I74 residues have been mutated to ionized residues to study the effect of electrostatic modifications to the channel.

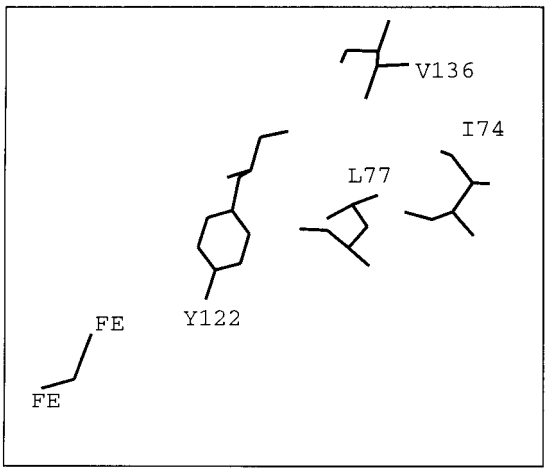

Figure 1. The relative positions of the tyrosyl radical, Y122, the diiron center, and the three mutations points, I74, L77, and V136. The atomic coordinates were taken from ref 13.

Table 1. Nature and Size of the Mutations and Their Distances from the Y122 Phenolic Oxygen[a]

mutant	type	$r_{O-C\alpha}$	side chain length[b]	r_{min}	r_{max}
I74R	neutral to charge	12.1	7.3	4.8	19.4
I74K	neutral to charge	12.1	6.2	5.9	18.3
I74F	steric	12.1	5.0	7.1	17.1
L77F	steric	7.2	5.0	2.3	12.3
V136R	neutral to charge	14.3	7.3	7.0	21.6
V136N	neutral to charge	14.1	3.7	10.4	17.8

[a] The distances from the tyrosyl oxygen atom to the α-carbon atom of the point of mutation, $r_{O-C\alpha}$, were taken from the crystallographic structure,[13] r_{max} and r_{min} represent the range of side chain to the phenolic oxygen distances that are possible. All distances are expressed in Å. [b] Fully extended.

In this study, we examine the effect of the mutations on the HF-EPR spectrum of the *E. coli* ribonucleotide reductase tyrosyl radical. In particular, the effects of changing the neutral residues I74 and V136 to charged ones within the hydrophobic channel are investigated. Two different electrostatic effects were anticipated. The first was the direct effect of introducing a charged group and the second the structural modification of the arrangement of the tyrosyl radical relative to the diiron center. Figure 1 shows the relative arrangement of the tyrosyl radical, diiron center, and the points of mutations. In Table 1, the distances from the phenolic oxygen of the radical to the α-carbon atoms of the mutation points are tabulated along with estimates of maximum lengths of the side chains. In all three neutral-to-charged mutants, the charged side chain can come within 7 Å of the tyrosyl radical; at such a distance a small but experimentally measurable shift in g-anisotropy is predicted.

The g-anisotropy of the RNR tyrosyl radical is likely to be affected by the nearest iron atom and its ligand.[5a] For example, the RNR tyrosyl radical from *Mycobacterium tuberculosis* has a slightly larger g-anisotropy than that of the *E. coli* protein indicating that the *M. tuberculosis* radical is likely to be

(10) Stone, A. J. *Proc. R. Soc. A* **1963**, *271*, 424−434. Stone, A. J. *Mol. Phys.* **1963**, *6*, 509−515. Stone, A. J. *Mol. Phys.* **1964**, *6*, 316.

(11) Knüpling, M.; Törring, J. T.; Un, S. *Chem. Phys.* **1997**, *219*, 291−304.

(12) Pimentel, G. C.; McClellan, A. L. *The Hydrogen Bond*; W. H. Freeman: London, 1960; pp 161−162.

(13) Nordlund, P.; Eklund, H. *J. Mol. Biol.* **1993**, *232*, 123.

(14) Gerez, C.; Elleingand, E.; Kauppi, B.; Eklund, H.; Fontecave, M. *Eur. J. Biochem.* **1997**, *249*, 401−407.

displaced further from the iron than in *E. coli*.[7b,c] Marked differences in microwave power saturation of the EPR resonances support this hypothesis. The *M. tuberculosis* radical saturates much more readily than its *E. coli* counterpart.[7b,c] A further evidence of the importance of the electrostatic influence of the diiron center on the tyrosyl *g*-values comes from the recent HF-EPR study of the tyrosyl radical generated by γ-irradiation of *N*-acetyltyrosine crystals.[15] The g_x value was found to be 2.0094 compared to 2.0089 for the *E. coli* RNR radical.[5,15] Since within the molecular crystal no electrostatic interactions are expected, this value can be taken as the "isolated" case. The lower value of the *E. coli* RNR radical is clearly due to the nearby diiron center.[16]

In the case of the mutants, there is no way to distinguish the direct effect of mutations from that of the iron. Changes in *g*-values will necessary reflect the total change in the electrostatic environment. Therefore, the unambiguous assignment of changes specifically due to the charged residues is not possible from the *g*-values. Hence, the changes in *g*-values will be analyzed in the context of both effects.

The study of the sensitivity of *g*-values to electrostatic effects has important consequences to a variety of HF-EPR applications. The protein electrostatic environment clearly plays an important role in determining the stability of radicals within the protein. A prime example of this is the difference between the two tyrosyl radicals in PSII. One radical is stable and is not involved in the primary electron transfer pathway and the second is short-lived and an integral component of electron transfer. The protein electrostatic environment presumably plays an important role in the electrochemical properties of the radical. As demonstrated in previous studies,[5−7] *g*-values can provide important insights into protein−radical interactions. Hence, a quantitative understanding of the sensitivity of *g*-values to these interactions is important. Another area of importance is the RNR, itself. Since the tyrosyl radical is essential for enzyme activity, it has been the target of various drugs.[17] For effective drug design, an understanding of the electrostatic interaction between the radical and protein is essential. Hence, HF-EPR measurements can provide valuable information in this regard.

Experimental Section

Protein Preparation. The *E. coli* R2 mutants have been constructed and prepared as previously described.[14] As the mutant proteins were partly or completely obtained in the apoprotein form after purification, reconstitution of the iron−radical center was achieved. First, proteins, 100 μM in 200 μL final volume, were incubated anaerobically inside a glovebox (Jacomex BS531 NMT) with a 4-fold molar excess of Fe-$(NH_4)_2(SO_4)_2$ in Tris-HCl (50 mM, pH 7.6), for 10 min. The samples were then transferred into EPR tubes and exposed to oxygen for 2−5 min, mixed well, and immediately frozen with liquid nitrogen.

High-Field EPR. The local-built high-field EPR spectrometer has been previously described.[6a] In this study, we have made extensive use of the manganese/magnesium oxide (Mn(II)/MgO) standard (g = 2.00101).[18] We carried out a series of calibration experiments to determine the reproducibility and accuracy of *g*-value measurement by repeatedly measuring the Mn(II)/MgO standard and RNR samples. Errors in *g*-value measurements were dominated by measurements in the magnetic field. The frequency of the phase-locked microwave source was known to better than 1 ppm. The apparent *g*-value of the standard could be readily determined to within $\pm 1 \times 10^{-5}$. Hence, the magnetic field could be calibrated to this accuracy. The reproducibility of a *g*-value measurement for a given protein sample was determined to be no worse than $\pm 4 \times 10^{-5}$. The linearity of the field sweep was verified by simulation of the six-line Mn(II)/MgO spectrum. The error due to the nonlinearity of the field-sweep was estimated to be no greater than the *g*-value determination, $\pm 1 \times 10^{-5}$. All spectra were taken under nonsaturating conditions. For a given sample, spectra were obtained over a decade power range to ensure that the line shapes were free of distortion and the signal amplitude scaled properly with microwave power. The field modulation amplitudes are specified as peak-to-peak and determined by using the same Mn/MgO standard. The modulation fields were sufficiently small (6 to 10 G) to ensure that line shapes were not distorted.

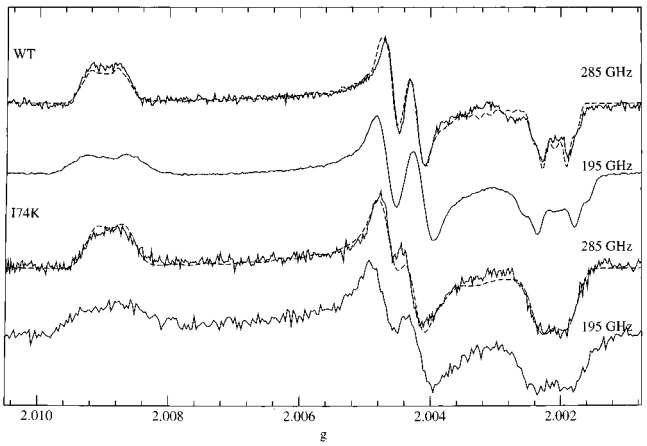

Figure 2. 285 and 190 GHz EPR spectra (solid lines) of the wild-type (upper) and I74K mutant (lower) of *E. coli* ribonucleotide reductase plotted as a function of *g*-value and 285 GHz simulations (dashed lines). Differences between the 285 and 190 GHz spectra for each tyrosyl radical are due to hyperfine interactions.

Simulation. Second-order perturbation equations were used to calculate the spectrum.[19] Two completely anisotropic and four isotropic hyperfine tensors were included in the spectrum calculations. The values and orientations of the hyperfine intetractions were taken from the work of Bennati and co-workers[20] and kept fixed leaving the three *g*-values as fitting parameters. The powder spectra were generated by summing the resonance field of 10^5 randomly chosen orientations of the magnetic field with respect to *g*-axis systems, followed by convolution with a derivative Gaussian function of suitable width and normalization to the experimental spectrum. The spectra were fitted by using standard conjugate gradient techniques.[21] The *g*-values obtained from the fitting procedure were tested to ensure that they were reliable to at least $\pm 1 \times 10^{-4}$. When the *g*-values obtained from the minimization procedure were intentionally shifted by $\pm 1 \times 10^{-4}$, the root-mean-square difference between experimental and simulated spectra increased by 5 to 10%. Re-minimization starting from the shifted values yielded *g*-values that were essentially identical to the original, confirming the reliability of the reported values.

Results

The 285 and 190 GHz EPR spectra of the wild-type (WT) and isoleucine-74 to lysine (I74K) mutant are shown in Figure 2 with a horizontal *g*-axis. The differences between the spectra taken at the two different frequencies arise from hyperfine couplings which are independent of the applied magnetic field.

(15) Mezzetti, A.; Maniero, A. L.; Brustolon, M.; Giacometti, G.; Brunel, L.-C. *J. Phys. Chem. A* **1999**, *103*, 9636−9643.

(16) In *E. coli* RNR, the nearest charged residues are further than 14 Å away from the oxygen of tyrosyl radical compared to the 5.3 Å of the nearest iron.

(17) For example see: Fontecave, M.; Lepoivre, M.; Elleingand, E.; Gerez, C.; Guittet, O. *Febs. Lett.* **1998**, *421*, 277−279.

(18) Burghaus, O.; Plato, M.; Rohrer, M.; Möbius, K.; MacMillan, F.; Lubitz, W. *J. Phys. Chem.* **1993**, *96*, 7639−7647.

(19) Pilbrow, J. R.; Winfield, M. E. *Mol. Phys.* **1973**, 25, 1073−1092.

(20) Bennati, M.; Farrar, C. T.; Bryant, J. A.; Inati, S. J.; Weis, V.; Gerfen, G. J.; Riggs-Gelasco, P.; Stubbe, J.; Griffin, R. G. *J. Magn. Reson.* **1999**, *138*, 232−243.

(21) Press, W. H.; Flannery, B. P.; Teukolsky, S. A.; Vetterling W. T. In *Numerical Recipe*; Cambridge University Press: New York, 1986.

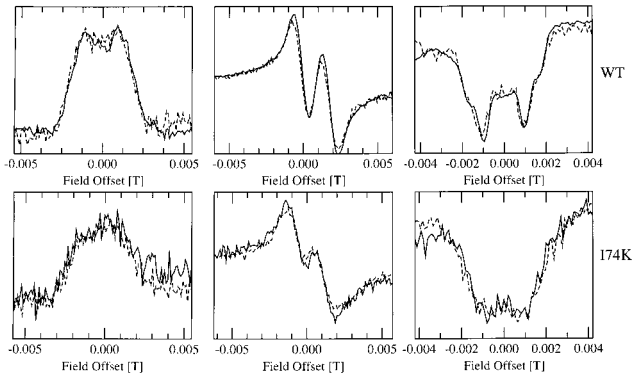

Figure 3. The g_x (left), g_y (middle), and g_z (right) regions of the 285 (dashed lines) and 190 (solid lines) GHz EPR spectra of the wild-type (upper panels) and I74K mutant (lower panels) plotted as a function of magnetic field. For each region, the spectra have been offset in field to achieve maximum overlap.

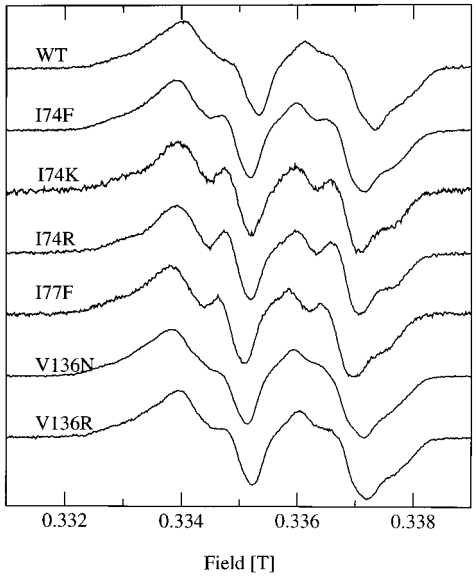

Figure 4. 9 GHz EPR spectra of the tyrosyl radicals in wild-type and mutants of *E. coli* ribonucleotide reductase. The spectra were taken under nonsaturating conditions. Sample temperature 10 K, microwave power 100 uW, modulation amplitude 2 G, and modulation frequency 100 kHz.

In Figure 3, each of the three turning points of the spectra, which correspond to the three principal *g*-values, are plotted with the horizontal magnetic field axes. When plotted in this fashion, within the signal-to-noise ratio, no difference can be seen for either the WT or I74K mutant. This indicates that the spectral resolution was limited by hyperfine couplings and not by the increase in magnetic field, since the former is independent of the applied magnetic field.

The spectra of the WT and the mutants could be adequately described by simulations (Figure 2) which fitted the *g*-values but fixed the hyperfine couplings to those which were recently determined by Bennati and co-workers[20] using high-field pulsed ENDOR for the *E. coli* wild-type RNR protein. This strongly suggests that there are no significant variations in the hyperfine couplings among the seven tyrosyl radicals. This is supported by two other observations. First, the 9 GHz spectra of the mutants and wild-type are nearly identical (Figure 4). Second, the splittings of the g_y feature in the 285 GHz spectra (Figures 5 and 6) are nearly the same. However, as demonstrated in Figures 2 and 3, the lower resolution observed for the I74K

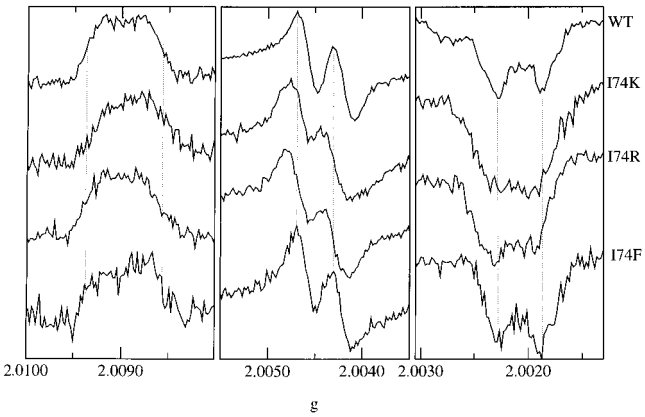

Figure 5. The g_x (left), g_y (middle), and g_z (right) regions of the 285 GHz EPR spectra of the wild-type and I74 mutants of *E. coli* ribonucleotide reductase plotted as a function of *g*-value.

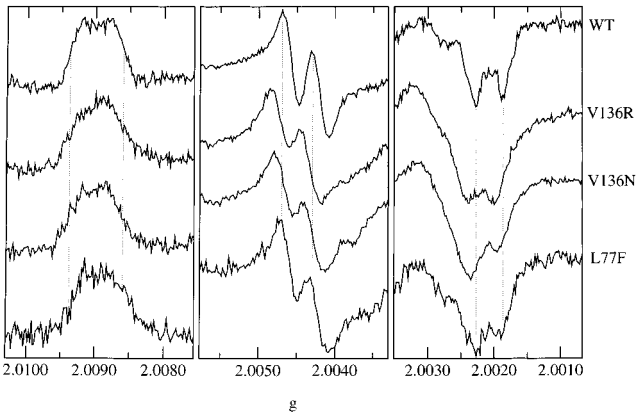

Figure 6. The g_x (left), g_y (middle), and g_z (right) regions of the 285 GHz EPR spectra of the wild-type and V136 and L77F mutants of *E. coli* ribonucleotide reductase plotted as a function of *g*-value.

mutant compared to that of the WT does arise from small differences or distribution in hyperfine couplings.

Figures 5 and 6 show the g_x, g_y, and g_z regions of the tyrosyl radical spectra from the I74 and V136 mutants. As expected, of the three I74 mutants (Figure 5), the phenylalanine (I74F) mutant most closely resembled the wild-type with identical *g*-values. Although somewhat noisy, the spectrum had comparable resolution to that of the native in all three regions of the spectrum. By comparison, the other two mutants exhibited marked differences from the wild-type. The g_z edge of the radical in the mutants was less resolved than that of the wild-type. The shape and position of the g_x edge of the isoleucine-74 to arginine (I74R) radical was comparable to those of wild-type; however, the I74K mutant had a measurable shift of -1×10^{-4} in the g_x position and overall shape was asymmetric and skewed toward lower values. The shift although small can be seen by direct visual comparison (Figures 2 and 5). This small shift is also reproduced by simulation (Table 2). It can be argued that the shift may be due to an error in measurement of the absolute field. The accuracy and reproducibility of the field calibration show that this is not the case. Moreover, the *g*-anisotropy, defined by $|g_x - g_z|$, is also clearly smaller for the I74R mutant compared to the wild-type. The accuracy in *g*-anisotropy does not rely on the absolute field. Due to the quality of the 190 GHz I74K spectrum and the inherently reduced *g*-resolution at the lower frequency, we were unable to detect the shift observed at 285 GHz. The apparent higher g_y values for the I74R and

Table 2. *g*-Values of the Tyrosyl Radicals in Wild-type and Mutant Proteins Obtained from Simulations[a]

	g_x	g_y	g_z
WT	2.00895	2.00438	2.00208
I74R	2.00888	2.00440	2.00205
I74K	2.00884	2.00438	2.00203
I74F	2.00891	2.00438	2.00203
L77F	2.00884	2.00430	2.00205
V136R[b]	2.00900	2.00444	2.00209
V136N[b]	2.00898	2.00449	2.00213

[a] The hyperfine couplings were kept fixed to those obtain by Bennati et al.[20] [b] g_y and g_z regions were obstructed by an overlapping radical that rendered simulations unreliable.

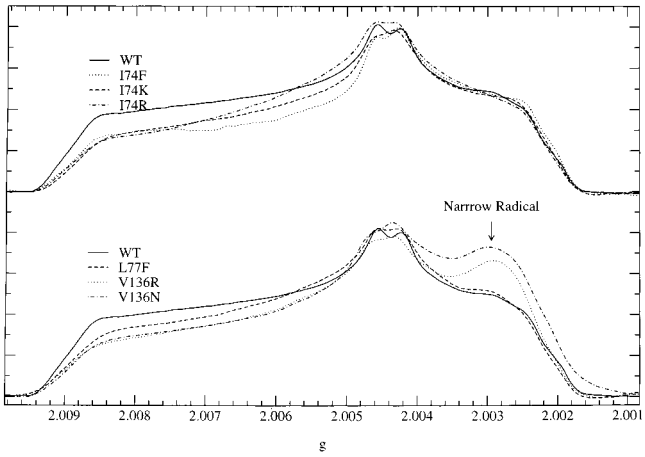

Figure 7. The integrated 285 GHz EPR spectra of the I74, L77, V136 mutant, and wild-type protein of *E. coli* ribonucleotide reductase. Each has been arbitrarily scaled so that intensity at the g_y value is the same.

I74K mutants compared to the wild-type were in fact due to greater inhomogeneous line width. This was verified by spectra obtained at 195 GHz and simulations (Figures 2 and Table 2). The I74F mutant spectrum, which exhibited slightly higher resolution, did not exhibit this shift.

The valine-136 to arginine (V136R) and asparagine (V136N) mutants also exhibited the same apparent g_y shift as observed for the I74R and I74K mutants (Figure 6). The g_x edge of the V136N mutant was identical with that of the wild-type. In the case of V136R, like the I74K mutant, the g_x portion of the spectrum was asymmetric. For both V136 mutants, a second much narrower contribution to the spectrum was observed. This contribution increased with time over several months. The approximate extent of the spectrum was from 2.0035 to 2.0020 (Figure 6). Also shown in Figure 6 is the spectrum of the tyrosyl radical in the leucine-77 to phenylalanine (L77F) mutant. Unlike the I74 phenylalanine mutant, the g_x value was shifted by approximately -1×10^{-4}.

The effects of the mutations described above are better visualized by using the normal absorption spectra rather than the customary field-derivative spectra. Figure 7 shows the HF-EPR absorption spectra of six mutants and wild-type obtained by integrating the corresponding derivative spectrum. For the I74 mutants, when the spectral regions between g_y and g_z are scaled to overlap with that of the wild type, the g_x-edges of the spectra of the mutants clearly differ from the wild-type rising less sharply. A shift in g_x value for isoleucine-74 to lysine mutant is also clearly visible. The presence of a second radical in the two valine-136 mutants is clearly visible in the absorption spectra.

Discussion

The EPR spectra of the RNR tyrosyl radical from different organisms exhibit a large range of *g*-values. For example, the RNR tyrosyl radicals in mouse and plant *(Arabidopsis thaliana*) have a g_x of about 2.0075. This low value has been interpreted to be due to a hydrogen bond to the radical.[7c,d] The tyrosyl radical in *M. tuberculosis* has a g_x value of 2.0092, which is higher than that of the *E.coli* radical. A 9 GHz microwave power saturation study indicated that the *M. tuberculosis* radical is readily saturable compared to the *E.coli* radical at 100 K.[7c] This observation taken together with the high g_x value suggested that the radical is likely to be further away from the iron in the case of *M. tuberculosis*. By comparison, the six mutations do not appear to have induced any large changes in *g*-values of the magnitude observed for the same proteins from different organisms. Therefore, we conclude that the mutations do not induce large-scale changes in the electrostatic environment of the tyrosyl radical. This conclusion is also supported by the fact that, with the exception of the valine-136 to arginine mutant, it was possible to obtain nonsaturated spectra at 10 K for the wild-type and the five other mutants. The V136R radical required a higher temperature of 30 to 40 K.

The differences among the HF-EPR tyrosyl radical spectra of the six mutants and the wild-type were small and subtle. The doublet g_z feature of the wild-type was not resolved in the I74K and I74R mutants. Multifrequency data (Figure 3) clearly show that this is due to hyperfine interactions. The most likely explanation is that in these two mutants the angular orientation of the β-proton with respect to the phenyl ring plane is distributed leading to a distribution of hyperfine couplings. The simultaneous loss in resolution at the g_y value is also consistent with this conclusion. On the basis of the resolution of the doublet g_y features, it is likely that the β-proton hyperfine interaction in the L77F, V136R, and V136N mutants is also distributed. However, the presence of an overlapping radical in the latter two mutants complicated analysis. The radical in I74F mutant appears to be the only case where the β-proton hyperfine interaction is as well defined as in the case of the wild-type radical.

The *g*-values for I74F mutant were also identical to those of wild-type indicating, as expected, that no change in the electrostatic environment occurred with this mutation. By comparison, the g_x value of L77F mutant was shifted by -1×10^{-4}, indicating that the radical in this case was in a slightly more electropositive environment. As the mutation to a phenylalanine residue does not introduce a charged group, the shift in *g*-value must be due to structural changes. Examination of the wild-type crystallographic structure indicated that no positively charged residues (lysines and arginines) are within 13 Å of the tyrosyl oxygen. Hence, the observed changes in *g*-values, and by implication the electrostatic potential at the oxygen, are likely to be due to reduction in the radical−metal distance. In the crystallographic structure of the L77F mutant, the tyrosyl is in fact 0.2 Å closer to the diiron center. However, at a resolution of 2.7 Å, it is not clear whether this small shift is significant. Semiempirical *g*-value calculations[5a,11] indicate that a g_x shift of 1×10^{-4} is consistent with a contraction of 0.2 Å.

The isoleucine-74 to lysine and to arginine mutants also exhibited differences. The g_x value of the I74K radical was shifted by -1×10^{-4} and the g_x edge was asymmetric. Simulations also indicated that the g_x value of the I74R radical is also shifted. However, experimental uncertainty and fitting errors make such a small shift difficult to assess. By contrast, the

downward shift observed for the I74K mutant could be directly measured from the spectrum (Figures 2, 5, and 7). Such a shift is consistent with the introduction of a positive charge near the tyrosyl oxygen and indicates that the lysine side chain extends toward the tyrosyl radical. The asymmetry of the g_x feature suggests that the electrostatic environment around the radical is distributed. The simplest explanation for this distribution is that the side chain is not uniquely positioned within the protein leading to a distribution in the charge−radical distance. Similarly, the valine-136 to arginine mutant radical also exhibited an asymmetric g_x edge presumably due to a distributed environment. The presence of a structural disorder in the isoleucine-74 and valine-136 mutants is supported by the observation that, with the exception of the isoleucine-74 to phenylalanine mutant, the hyperfine resolution in the g_y and g_z regions is lost in these mutants. This indicates that hyperfine interaction between the β-carbon protons and the unpaired electron is likely to be distributed due to disorder in the phenyl-ring plane orientation with respect to β-carbon protons.

The presence of a second radical in the V136 mutants is not too surprising. The tyrosyl radicals in both V136 mutants had shorter lifetimes (10 to 20 min) than all the other radicals (>8 h).[14] The spectrum of this second radical (Figure 7) is much narrower and is similar in extent to radicals observed in γ-irradiated tyrosyl crystals.[22] The 9 GHz spectrum of the V136R mutant did not show any evidence of this narrow radical when compared to the other spectra. There are two possibilities which could account for this. First, the hyperfine spectrum of this radical is sufficiently similar to that of the tyrosyl radical to render it indistinguishable at 9 GHz. This seemed unlikely. *g*-values are in part determined by ground-state spin density. Hence, large differences in *g*-values should also be reflected in hyperfine couplings. The second possible explanation is that 9 GHz spectrum of the unidentified radical is extremely broad. However, we found no indications of a broader radical. The identification of this radical will require further investigation. Nonetheless, the much narrower *g*-anisotropy clearly indicates that the radical is not a typical π-planar tyrosyl radical. If the radical is centered on the phenyl ring, the electronic structure of the ring must be different from a normal tyrosyl radical. One possibility is the partial loss of ring conjugation.[22] However, one would expect such a radical to be less stable than the aromatic radical. It is more likely that the radical is centered on another residue.

To appreciate the results of the present study in a global context, we have extended the simplified model that was first developed in our previous studies. We assume that the effect of the electrostatic potential imposed by the protein can be modeled by a single effective charge at a distance, *r*, from the phenolic oxygen. This is equivalent to truncating eq 2 to second order in r^{-1}. An important ingredient in this model is the recently measured *g*-anisotropy for the *N*-acetyltyrosyl radical. This radical is not hydrogen bonded and there are no charged groups within the molecular crystal. For this radical, the g_x is 2.0094. We note that this value was predicted based on our semiempirical calculations.[5b] This value is taken as the limiting case where the charge is an infinite distance away from the radical and is the zero-order term of eq 2. In the case of the *E. coli* ribonucleotide reductase, the integrated effect of all the charged groups near the tyrosyl radical can be replaced by an effective charge at a distance of 7 Å. This distance is longer than the phenoxyl oxygen to nearest iron distance of 5.2 Å due to the effects of the negatively charged ligands. The g_x value for the *E. coli* radical is 2.0090. Using this value, it is possible to estimate the second-order term of eq 2. This leads to

$$g_x = 2.0094 - \frac{0.0169}{(r - 0.50)^2} \qquad (3)$$

We have used a distance offset of 0.50 Å to be consistent with the expression previously obtained based on semiempirical calculations on the effect of an acetic acid hydrogen bond donor.[5b] Equation 3 is plotted in Figure 8. Along with eq 3, the theoretically calculated dependence of the tyrosyl g_x value on the hydrogen-bonding distance is also shown. This curve was determined from semiempirical molecular orbital calculations on a model system that consisted of a *p*-cresol radical hydrogen bonded by an acetic-acid molecule.[5a,b,11] We have also superimposed the experimentally measured g_x values of several other tyrosyl radicals, including those that are hydrogen bonded. For radicals involved in hydrogen-bonding, the apparent distance between oxygen and charge, predicted by eq 3, is longer than the actual oxygen and hydrogen-bond donor distance. This is because of the stronger electric effect of a single charge relative to a dipole of a hydrogen-bond donor. In the case of the tyrosine hydrochloride radical, the hydrogen donor can be crudely approximated by an electric dipole with a moment of 1.7 D,[23] the dipole moment of acetic acid, and the positive end 1.65 Å away from the phenoxyl oxygen, as in the crystal structure. The equivalent electrical distance for a single charge is about 2.9 Å, the same as that obtained from eq 3 for a g_x value of 2.0065. Hence, our simple model accounts for the three cases for which crystallographic information is available. It should be emphasized that this simple-charge model neglects angular effects, as well as complexities arising from variations in the local dielectric

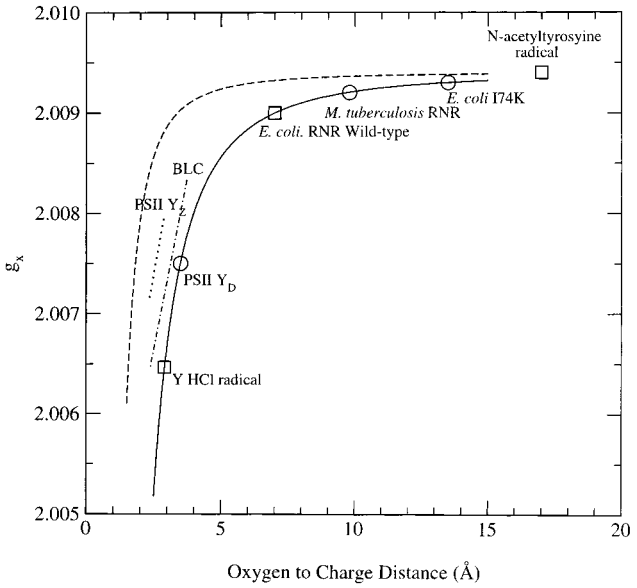

Figure 8. The effective charge model of the tyrosyl radical g_x value. The solid line is given by eq 3 and was determined from the values shown with square (□) symbols (see text). The dashed line is given by the expression $2.0094 - 0.0033(r - 0.05)^{-2}$ and describes the calculated g_x value of a *p*-cresol radical as a function of the hydrogen-bonding distance to an acetic acid molecule, as described in ref 5a,b. The dotted (•••) line represents the g_x values spanned by Y_Z of PSII[5b] and the dot−dashed (− • −) line by the tyrosyl radical in bovine liver catalase (BLC).[6]

(22) Fasanella, E. L.; Gordy, W. *Proc. Natl. Acad. Sci. U.S.A.* **1969**, *62*, 299−304.

(23) *Handbook of Chemistry and Physics*; Lide, D. R., Ed.; CRC Press: New York, 1996.

constant. Hence, it represents a highly approximative picture, the main benefit of which is that it provides a means by which tyrosyl *g*-values can be compared and rationalized, as well as predicted based on structural information.

By using eq 3 and Figure 8, it is now possible to rationalize several other g_x values. A shift of 1×10^{-4} measured for the I74K mutant corresponds to a distance of about 13 Å, a reasonable value based on the wild-type structure (Table 1). The same g_x shift can also correspond to a contraction of the radical−charge distance from 7 Å (wild-type) to 6.3 Å for the mutants. For the two tyrosyl radicals which exhibit distributed g_x values, Y_z of PSII and BLC, the distribution in *g* corresponds to a distribution distance of about 0.5 to 1 Å. For hydrogen bonds, this represents a large distance range. The hydrogen-bonding effect is also orientation dependent and some part of the large g_x-distribution may also be due to disorder in the hydrogen-bond angles.[5b]

Implicit in the above discussion of the simple-charge model is the fact that the effect of positively charged groups, such as metal center, lysine, and arginine residues, and hydrogen bonds cannot be differentiated by a *g*-value measurement. The two curves shown in Figure 8 cannot be differentiated on the basis of a single measurement. Without additional information, *g*-values cannot be used as an indicator of hydrogen bonding, especially when other ionic groups are present. Because the *g*-anisotropy reflects the sum of all electrostatic contributions of the protein, it is conceivable that a nearby negatively charged residue could mask the presence of a hydrogen bond.

Using our simple charge model, we have examined some recent results reported for the RNR tyrosyl radical from *M. tuberculosis*. The model predicts that the effective charge distance for the tyrosine radical in this protein is 10 Å, 3 Å longer than in *E. coli*. A recent modeling study based on the structure of *Salmonella typhimurium*[7e] suggests that the distance from the phenoxyl oxygen to nearest iron distance is 7 Å. As with the *E. coli* benchmark value, the effective charge distance is likely to be longer than the actual distance due to the negatively charged ligands. Therefore, eq 3 appears to yield results roughly consistent with the modeling study.

A recent HF-EPR study of the *M. tuberculosis* protein has suggested that the radical exists in a heterogeneous environment.[7a] Freshly reconstituted protein exhibited a high-field spectrum with two g_x edge features as well as broadened g_y and g_z features. The g_x values were 2.0092 and 2.0080. Repeated freezing and thawing yielded a single broad g_x feature. These results were interpreted as two populations distinguished by the absence (2.0092) and presence (2.0080) of a hydrogen bond. Unfortunately, these HF-EPR results are equivocal due to the nature of the data. A survey of high-field measurements clearly indicates that the g_y is far less sensitive to electrostatic effects and the g_z values are essentially constant.[24] This is consistent with theoretical predictions. However, the published spectra show considerable broadening or additional features in both the g_y and g_z regions possibly indicating artifacts due to microwave power saturation or magnetic-field inhomogeneity. Assuming these problems do not affect the measurement of the g_x-values, the relatively high g_x-value of 2.0080 indicates the hydrogen bond must be weaker than in photosystem II (2.0075). The simple charge model predicts an effective distance of 4.0 Å compared to 3.5 Å. HF-EPR and 9 GHz ENDOR studies indicate that the hydrogen-bonding distance, defined as phenoxyl oxygen to donor proton distance, in PSII is about 1.7 to 1.8 Å. This implies that in the *M. tuberculosis* protein the distance must be greater, at least 2 Å. Presumably, such a hydrogen bond would be extremely weak.[6a] An alternative which has not been considered is that the distance between the radical and iron center has contracted leading to a reduction in the g_x-value. Solely based on the HF-EPR data, it would be difficult to distinguish between these two possibilities.

Conclusion

From the results of this and other studies, it is clear that the *g*-values of tyrosyl radicals are sensitive to even relatively weak electrostatic perturbations. For π-radicals with significant spin-densities on oxygen atoms, such as semiquinones, or nitrogens, such as flavosemiquinones, the underlying quantum mechanics which determines the *g*-anisotropy is likely to be the same as that for tyrosyl radical. Therefore, such radicals are also likely to be equally sensitive. We have shown that the *g*-values of the ribonucleotide reductase tyrosyl radical are sensitive to mutations which are relatively distant from the site of the radical. This study clearly demonstrates that the precisely measured *g*-values of tyrosyl radicals can be used as a powerful probe of the electrostatic environment induced by the protein on the radical.

Acknowledgment. We thank B. Kauppi and Prof. H. Norlund for supplying the coordinates of the L77F crystallographic structure. S.U. gratefully acknowledges Pierre Dorlet and Anabella Ivancich for assistance and helpful discussions. This research was supported by grants from the Human Frontier Science Organization (Contract RGO249) and the Region Ile-de-France (Contract Sesame).

JA003650B

(24) For examples see refs 5, 6, and 7.